Flow of a Second-Order Fluid Between Two Infinite Discs in the Presence of Transverse Magnetic Field

Reshu Agarwal[#1], Deepak Agarwal[*]

 # Assistant Prof (Senior Scale), Department of Mathematics, University of Petroleum and Energy Studies, Dehradun, India

** Associate Prof, Department of Mathematics, GRD Girls Degree College, Dehradun, India*

Abstract – *In this problem the flow of an incompressible second-order fluid confined between two infinite parallel discs under the transverse magnetic field, one stationary (stator) and other rotating (rotor), has been considered when there is a uniform injection normal to the stator. The solution of the problem is sought by expanding all the flow functions in the ascending powers of Reynolds numbers (assumed small). The effects of the elastico-viscosity τ_1, cross-viscosity τ_2, Reynolds number R, magnetic field m_1 and injection k on the velocity profile have been investigated and their behaviour have been shown graphically. Shearing stress at rotor and stator has also been calculated.*

Keywords – *Second order fluid, infinite discs, Magnetic Field*

I. INTRODUCTION

The phenomenon arising out of the flow between two discs has important applications in chemical and mechanical engineering as its generalization could be helpful in the study of heat transfer for analysis of air cooling of turbine discs and the determination of oil film temperature of pedestal bearing with centre feeding of lubricant. Several authors have discussed the steady flow of an incompressible viscous fluid between two infinite rotating discs theoretically as well as experimentally. Sharma & Gupta [1] have considered a general case of the flow of a non-Newtonian second-order fluid between two infinite torsionally oscillating discs. Rajgopal [2] studied the flow of a second-order fluid between rotating parallel plates. Sharma & Singh [3] have considered the forced flow of a second-order fluid between two porous discs. Sadhna Kahre [4] studied the steady flow between a rotating and porous stationary disc in the presence of transverse magnetic field. B. B. Singh and Anil Kumar [5] have considered the flow of a second-order fluid due to the rotation of an infinite porous disc near a stationary parallel porous disc.

In our present problem, we here study the flow pattern of an incompressible second-order fluid between two parallel infinite discs in the presence of transverse magnetic field when one is rotating (called rotor) and other is at rest (called stator). A uniform injection is applied to the stator forming the subject matter of the paper. The rotor coincides with the plane z = 0 and the stator coincides with the plane z = d. Here the dimensionless parameters $\tau_1(=\mu_2/\rho d^2)$, $\tau_2(=\mu_2/\rho d^2)$ govern the effects of elastico-viscosity and cross-viscosity, while the effects of the injection are governed by a non-dimensional parameter $k(=w_0/2d\Omega)$ where w_0 is the uniform suction velocity (negative for injection).

II. BASIC EQUATION

The constitutive equation of an incompressible second-order fluid as suggested by Coleman and Noll [6] can be written as:

$$\tau_{ij} = - p\delta_{ij} + 2\mu_1 d_{ij} + 2\mu_2 e_{ij} + 4\mu_3 c_{ij} \qquad (1)$$

where

$$d_{ij} = \tfrac{1}{2}(u_{i,j} + u_{j,i}),$$

$$e_{ij} = \tfrac{1}{2}(a_{i,j} + a_{j,i}) + u^m{}_{,i}u_{m,j},$$

$$c_{ij} = d_{im}\, d^m{}_{,j}. \qquad (2)$$

p is the hydro-static pressure; τ_{ij} is the stress-tensor; u_i and a_i are the velocity and acceleration vector; μ_1, μ_2, μ_3 are the mathematical constants and δij is Kronecker's delta.

The second-order fluid characterised by the equation (1) confined between two infinite discs. The disc coinciding with the plane z = 0 rotates with a uniform angular velocity Ω about z-axis, while the other (assumed porous) coincides with the plane z = d and is at rest. A uniform injection $-w_0$ (w_0 being positive in z-increasing direction) is applied normal to the rotating disc. The space between the rotating discs is occupied by homogeneous, electrically conducting, incompressible second-order fluid. Let us suppose that u, v, w are the velocities in r, θ and z directions respectively. Let us suppose that axes of the discs coincide with z-axis and the origin of the cylindrical co-ordinates is taken at the centre of the rotatory disc. Under transverse magnetic field of

constant intensity B, equation of motion, leaving induced magnetic fields, for steady flow are (cf. Srivastava [7] and Wilson & Schryer[8])

$\rho\{u(\partial u/\partial r)+w(\partial u/\partial z)-v^2/r\} = \partial\tau_{rr}/\partial r + \partial\tau_{rz}/\partial z + (1/r)(\tau_{rr} - \tau_{\theta\theta}) - \sigma B^2 u/\rho,$ (3)

$\rho\{u(\partial v/\partial r)+w(\partial v/\partial z)+uv/r\}= \partial\tau_{r\theta}/\partial r + \partial\tau_{\theta z}/\partial z + 2\tau_{r\theta}/r- \sigma B^2 v/\rho,$ (4)

$\rho\{u(\partial w/\partial r)+w(\partial w/\partial z)\} = \partial\tau_{rz}/\partial r + \partial\tau_{zz}/\partial z + \tau_{rz}/r$ (5)

Equation of continuity:

$\partial u/\partial r + u/r + \partial w/\partial z = 0$ (6)

where u, v, w are the radial, transverse and axial components of velocity respectively. ρ and σ are respectively density and the conductivity of the fluid considered. The relevant boundary conditions of the problem are:

$z = 0: \quad u = 0, \quad v = r\Omega, \quad w = 0,$

$z = d: \quad u = 0, \quad v = 0, \quad w = -w_0,$ (7)

The velocity components for axi-symmetric flow compatible with continuity criterion (6) can be taken as (cf. Von-Karman[9])

$u = r\Omega F'(\zeta),$

$v = r\Omega G(\zeta),$

$w = -2d\Omega F(\zeta).$ (8)

and

$P = \Omega\mu_1[-p_1(\zeta) + R\xi^2(2\tau_1+\tau_2)(F''^2+G'^2) + \lambda\xi^2].$ (9)

where $\zeta=z/d$, $\xi = r/d$, $R=\Omega\rho d^2/\mu_1$, $\tau_1 = \mu_2/\rho d^2$(elastico-viscosity), $\tau_2 = \mu_3/\rho d^2$ (cross-viscosity). Here the primes denote derivatives w.r.t. ζ And λ is an arbitrary constant to be determined from the boundary conditions (7).

In view of (8), the boundary conditions (7) become

$\zeta = 0: \quad F = 0, \quad G = 1, \quad F' = 0,$

$\zeta = 1: \quad F = k, \quad G = 0, \quad F' = 0,$ (10)

where $k = w_0/2d\Omega$ is a dimensionless parameter representing the injection of the stator.
Following sets of equations are obtained after substituting (8) & (9) into (1), (3), (4), (5)

$R(F'^2–2FF''-G^2) = F'''-2R\tau_1(F''^2+2G'^2+FF^{iv}) - R\tau_2(F''^2+ 3G'^2+2F'F''')+ m^2F'-2\lambda$ (11)

$2R(F'G-FG') = G''+2R\tau_1(F''G'-FG''')+2R\tau_2(F''G'-F'G'')-m^2G$ (12)

$4RFF' = p_1'-2F''+4R\tau_1(11F'F''+FF''')+28R\tau_2F'F''$ (13)

where $m^2 = B^2\sigma d^2/\mu_1$ is the dimensionless constant.

III. RESULTS AND CONCLUSION

The variation of radial velocity for different elastico-viscous parameter τ_1 = -1. 3, -2, -2.6; when cross-viscous parameter τ_2 = 10, injection parameter k = 5, Reynolds number R = 0.05, magnetic field m_1 = 5 is shown in fig (1). In this figure, the curve of radial velocity w.r.t. ζ is bell shaped and the radial velocity increases in the first half and then decreases in the second half of the gap-length. It is also evident from this figure that the radial velocity decreases with increase in τ_1 at ζ = 0.1, 0.2, then it begins increase with increase in τ_1 upto ζ = 0.7 and then decreases with increase in τ_1 at ζ = 0.8, 0.9. The value of radial velocity is approximately equal at ζ = 0.28 and ζ = 0.72 for all values of τ_1. The point of maxima is in the middle of the gap-length for all values of elastico-viscous parameter τ_1.

The variation of transverse velocity for different elastico-viscous parameter τ_1 = -1.3, -2, -2.6; when cross-viscous parameter τ_2 = 10, injection parameter k = 5, Reynolds number R = 0.05, magnetic field m_1 = 5 is shown in fig (2). In this figure, the transverse velocity increases upto ζ = 0.7 and increases thereafter. It is also evident from this figure that the transverse velocity decreases with increase in τ_1 throughout the gap-length.

The variation of axial velocity for different elastico-viscous parameter τ_1 = -1.3, -2, -2.6; when cross-viscous parameter τ_2 = 10, injection parameter k = 5, Reynolds number R = 0.05, magnetic field m_1 = 5 is shown in fig (3). In this figure, the axial velocity increases throughout the gap-length. It is also evident from this figure that the axial velocity decreases with increase in τ_1 in the first half and it increases with increase in τ_1 in the second half of the gap-length.

The variation of radial velocity for different cross-viscous parameter τ_2 = 3, 5, 7; when elastico-viscous parameter τ_1 = -1, injection parameter k = 5, Reynolds number R = 0.05, magnetic field m_1 = 5 is shown in fig (4). In this figure, the curve of radial velocity w.r.t. ζ is bell shaped and the radial velocity increases in the first half and then decreases in the second half of the gap-length. It is also evident from this figure that the radial velocity decreases with increase in τ_2 at ζ = 0.1, 0.2, then it begins increase with increase in τ_2 upto ζ = 0.7 and then decreases with increase in τ_2 at ζ = 0.8, 0.9. The value of radial velocity is approximately equal at ζ = 0.278

and $\zeta = 0.722$ for all values of τ_2. The point of maxima is in the middle of the gap-length for all values of cross-viscous parameter τ_2.

The variation of transverse velocity for different cross-viscous parameter $\tau_2 = 3, 5, 7$; when elastico-viscous parameter $\tau_1 = -1$, injection parameter $k = 5$, Reynolds number $R = 0.05$, magnetic field $m_1 = 5$ is shown in fig (5). In this figure, the transverse velocity increases upto $\zeta = 0.7$ and decreases thereafter. It is also evident from this figure that the transverse velocity decreases with increase in τ_2 at $\zeta = 0.7$ and then increases with increase in τ_2.

The variation of axial velocity for different cross-viscous parameter $\tau_2 = 3, 5, 7$; when elastico-viscous parameter $\tau_1 = -1$, injection parameter $k = 5$, Reynolds number $R = 0.05$, magnetic field $m_1 = 5$ is shown in fig (6). In this figure, the axial velocity increases throughout the gap-length. It is also evident from this figure that the axial velocity decreases with increase in τ_2 in the first half and it increases with increase in τ_2 in the second half of the gap-length.

The variation of radial velocity for different injection parameter $k = 3, 5, 6$; when elastico-viscous parameter $\tau_1 = -0.4$, cross-viscous parameter $\tau_2 = 2$, Reynolds number $R = 0.05$, magnetic field $m_1 = 5$ is shown in fig (7). In this figure, the curve of radial velocity w.r.t. ζ is bell shaped and the radial velocity increases in the first half and then decreases in the second half of the gap-length. It is also evident from this figure that the radial velocity decreases with increase in injection parameter throughout the gap-length. The point of maxima is in the middle of the gap-length for all values of injection parameter k.

The variation of transverse velocity for different injection parameter $k = 3, 5, 6$; when elastico-viscous parameter $\tau_1 = -0.4$, cross-viscous parameter $\tau_2 = 2$, Reynolds number $R = 0.05$, magnetic field $m_1 = 5$ is shown in fig (8). In this figure, the transverse velocity increases upto $\zeta = 0.6$ and decreases thereafter. It is also evident from this figure that the transverse velocity increases with increase in injection parameter k throughout the gap-length.

The variation of axial velocity for different injection parameter $k = 3, 5, 6$; when elastico-viscous parameter $\tau_1 = -0.4$, cross-viscous parameter $\tau_2 = 2$, Reynolds number $R = 0.05$, magnetic field $m_1 = 5$ is shown in fig (9). In this figure, the axial velocity increases throughout the gap-length. It is also evident that it also increases with increase in injection parameter k throughout the gap-length.

The variation of radial velocity for different Reynolds number $R = 0.01, 0.06, 0.09$; when elastico-viscous parameter $\tau_1 = -0.4$, cross-viscous parameter $\tau_2 = 2$, injection parameter $k = 4$, magnetic field $m_1 = 5$ is shown in fig (10). In this figure, the curve of radial velocity w.r.t. ζ is bell shaped and the radial velocity increases in the first half and then decreases in the second half of the gap-length. It is also evident from this figure that the radial velocity decreases with increase in Reynolds number R at $\zeta = 0.1, 0.2$, then it begins increase with increase in Reynolds number R upto $\zeta = 0.7$ and then decreases with increase in Reynolds number R at $\zeta = 0.8, 0.9$. The value of radial velocity is approximately equal at $\zeta = 0.28$ and $\zeta = 0.72$ for all values of Reynolds number R. The point of maxima is in the middle of the gap-length for all values of Reynolds number R.

The variation of transverse velocity for different Reynolds number $R = 0.01, 0.06, 0.09$; when elastico-viscous parameter $\tau_1 = -0.4$, cross-viscous parameter $\tau_2 = 2$, injection parameter $k = 4$, magnetic field $m_1 = 5$ is shown in fig (11). In this figure, the transverse velocity decreases throughout the gap-length. It is also evident from this figure that the transverse velocity decreases with increase in R at $\zeta = 0.1$ and then increases with increase in R.

The variation of axial velocity for different Reynolds number $R = 0.01, 0.06, 0.09$; when elastico-viscous parameter $\tau_1 = -0.4$, cross-viscous parameter $\tau_2 = 2$, injection parameter $k = 4$, magnetic field $m_1 = 5$ is shown in fig (12). In this figure, the axial velocity increases throughout the gap-length. It is also evident from this figure that the axial velocity decreases in the first half and increases in the second half of the gap-length.

The variation of radial velocity for different magnetic field $m_1 = 1, 10, 15$; when elastico-viscous parameter $\tau_1 = -0.4$, cross-viscous parameter $\tau_2 = 2$, injection parameter $k = 4$, Reynolds number $R = 0.05$ is shown in fig (13). In this figure, the curve of radial velocity w.r.t. ζ is bell shaped and the radial velocity increases in the first half and then decreases in the second half of the gap-length. It is also evident from this figure that the radial velocity decreases with increase in magnetic field m_1 at $\zeta = 0.1, 0.2$, then it begins increase with increase in magnetic field m_1 upto $\zeta = 0.7$ and then decreases with increase in magnetic field m_1 at $\zeta = 0.8, 0.9$. The value of radial velocity is approximately equal at $\zeta = 0.28$ and $\zeta = 0.72$ for all values of magnetic field m_1. The point of maxima is in the middle of the gap-length for all values of magnetic field m_1.

The variation of transverse velocity for different magnetic field $m_1 = 1, 10, 15$; when elastico-viscous parameter $\tau_1 = -0.4$, cross-viscous parameter $\tau_2 = 2$, injection parameter $k = 4$, Reynolds number $R = 0.05$ is shown in fig (14). In this figure, the transverse velocity decreases throughout the gap-length. It is also evident that the transverse velocity decreases with increase in magnetic field m_1.

The variation of axial velocity for different magnetic field m_1 = 1, 10, 15; when elastico-viscous parameter τ_1 = -0.4, cross-viscous parameter τ_2 = 2, injection parameter k = 4, Reynolds number R = 0.05 is shown in fig (15). In this figure, the axial velocity increases throughout the gap-length. It is also evident from this figure that the axial velocity decreases with increase in magnetic field m_1 in the first half and it increases with increase in magnetic field m_1 in the second half of the gap-length. The transverse shearing stress on the lower and upper disc is

$(\tau_{\theta z})_{z=0}$ = -1+R{k-2k(τ_1+τ_2)-m_1^2/3} + R^2[-761k^2/3150-3/700+{24k^2(τ_1+τ_2)/5 + m_1^2k/10}(1/140)+k^2(τ_1+τ_2)/5 +m_1^2k/15- 2τ_1{76361k^2/47775+ {24k^2(τ_1+τ_2)/5 +m_1^2k/10} (9/4)+22k^2(τ_1+τ_2)/5+13m_1^2k/30}- 2τ_2{2k^2(τ_1+τ_2)-367k^2/2940+22m_1^2k/39}–551m_1^2k/4200+ m_1^2k(τ_1+τ_2)/30+m_1^4/45],

and

$(\tau_{\theta z})_{z=z0}$ = -1-27Rk/10- 2kR(τ_1+τ_2)+m_1^2R/6+ R^2[3061k^2/3150+2/1575+ {24k^2(τ_1+τ_2)/5+m_1^2k/10} (5883/420)+k^2(τ_1+τ_2)/5-2m_1^2k/15+ 2τ_1{199859k^2/47775+{24k^2(τ_1+τ_2)/5+m_1^2k/10}(27/4)+ 38k^2(τ_1+τ_2)/5+17m_1^2k/30}-2τ_2{613k^2/2940+2k^2(τ_1+τ_2)-14m_1^2k/39}+337m_1^2k/2100+ m_1^2k(τ_1+τ_2)/30-7m_1^4/360]. respectevily.

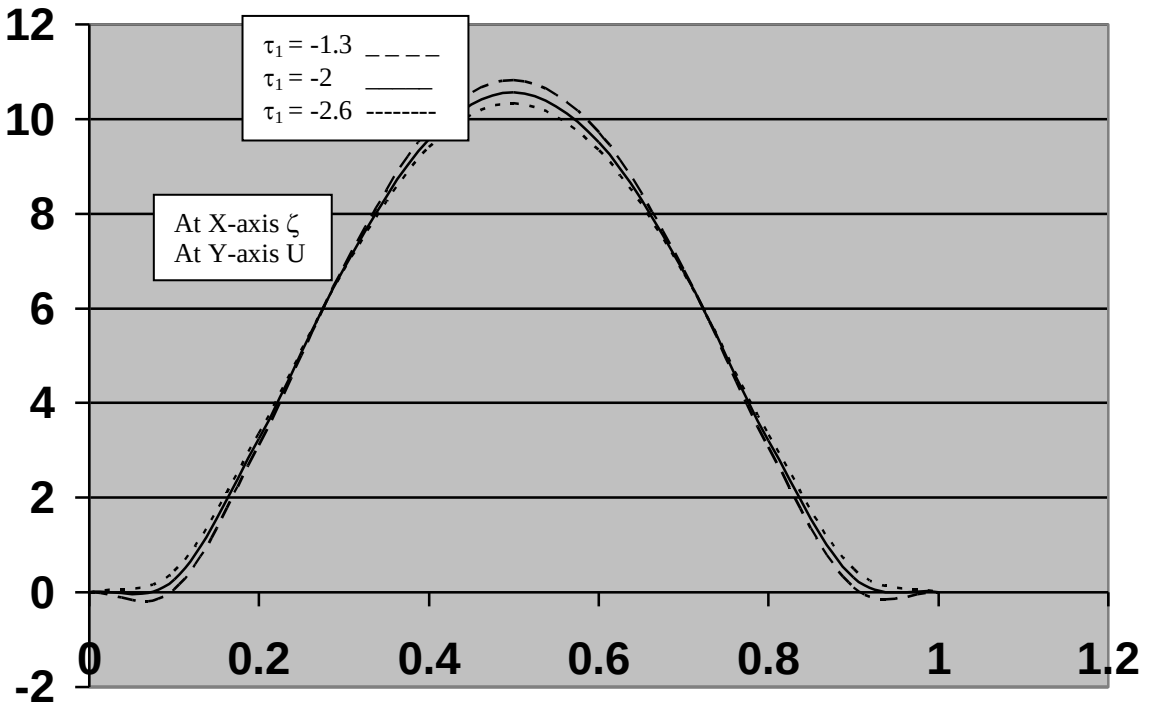

Fig.1 Response of radial velocity to an increase in cross-viscous effects.

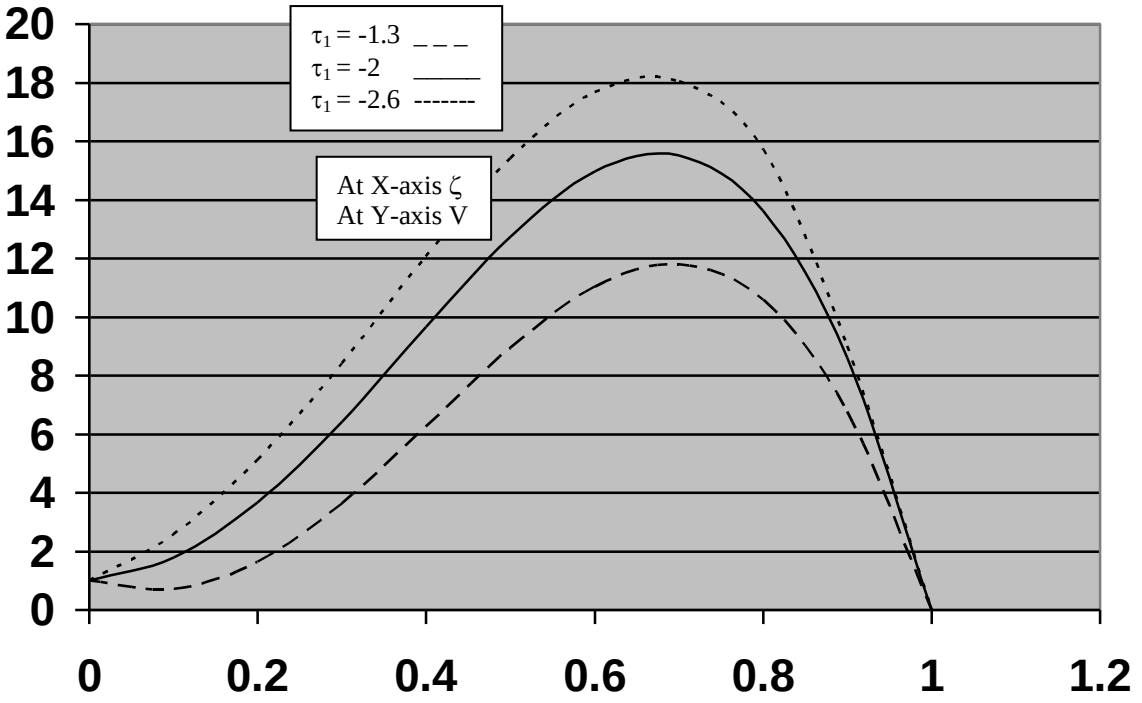

Fig.2 Response of transverse velocity to an increase in cross-viscous effects.

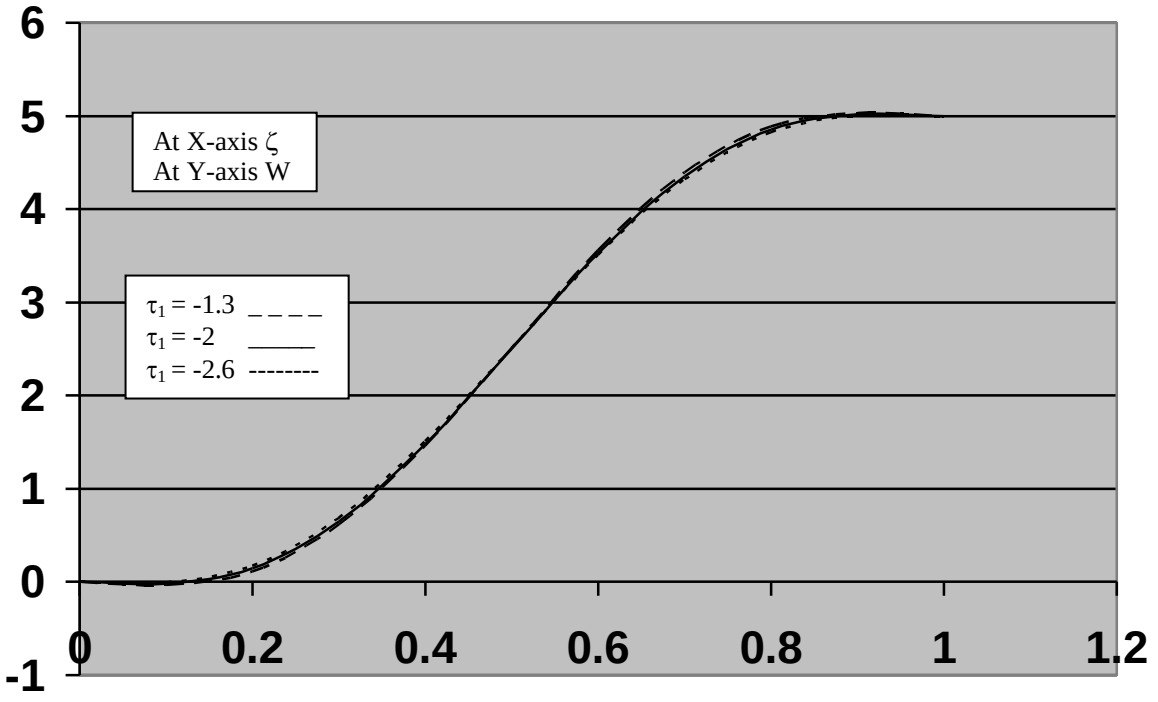

Fig.3 Response of axial velocity to an increase in cross-viscous effects.

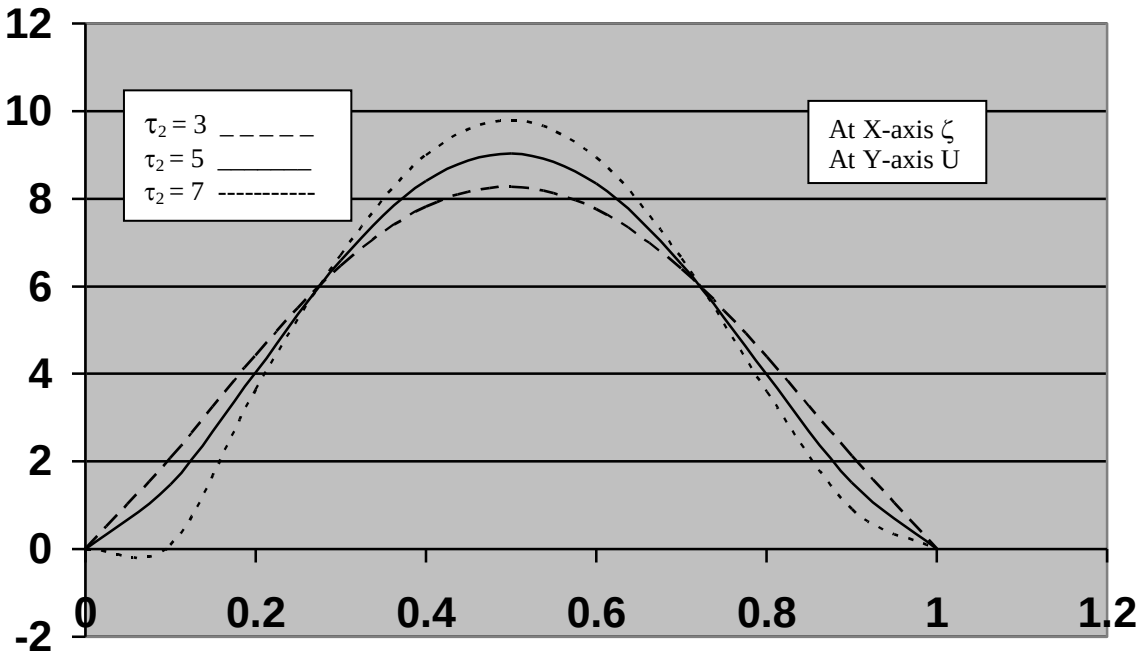

Fig. 4 Response of radial velocity to an increase in elastico-viscous effects.

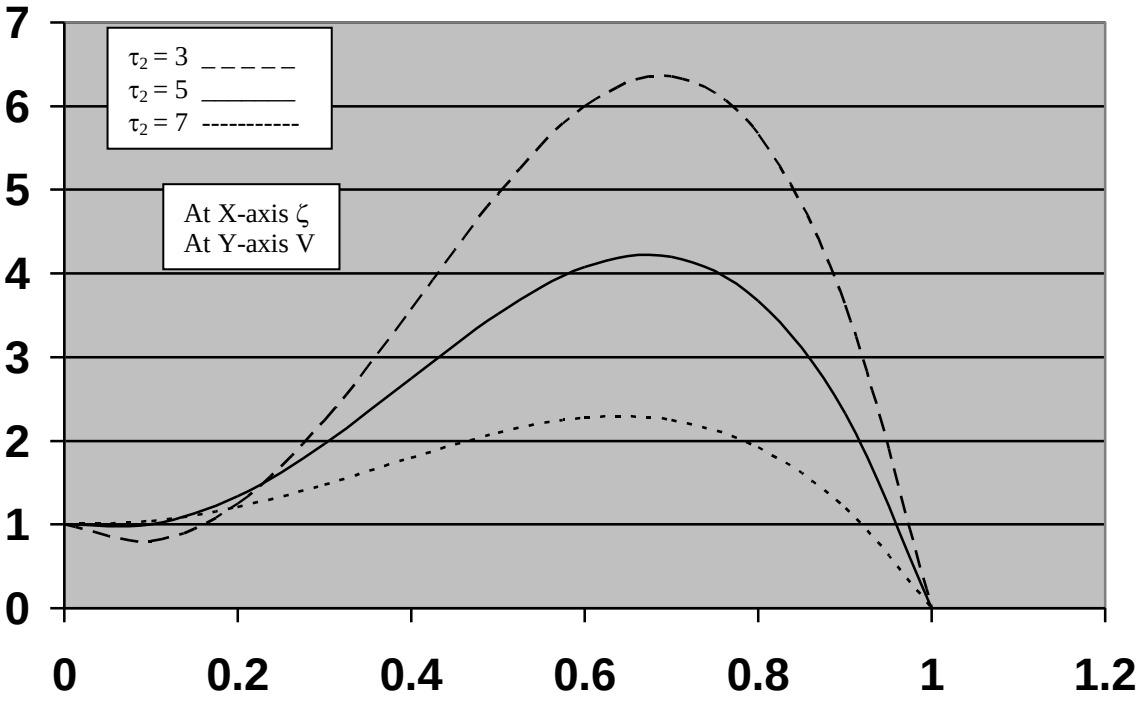

Fig.5 Response of transverse velocity to an increase in elastico-viscous effects.

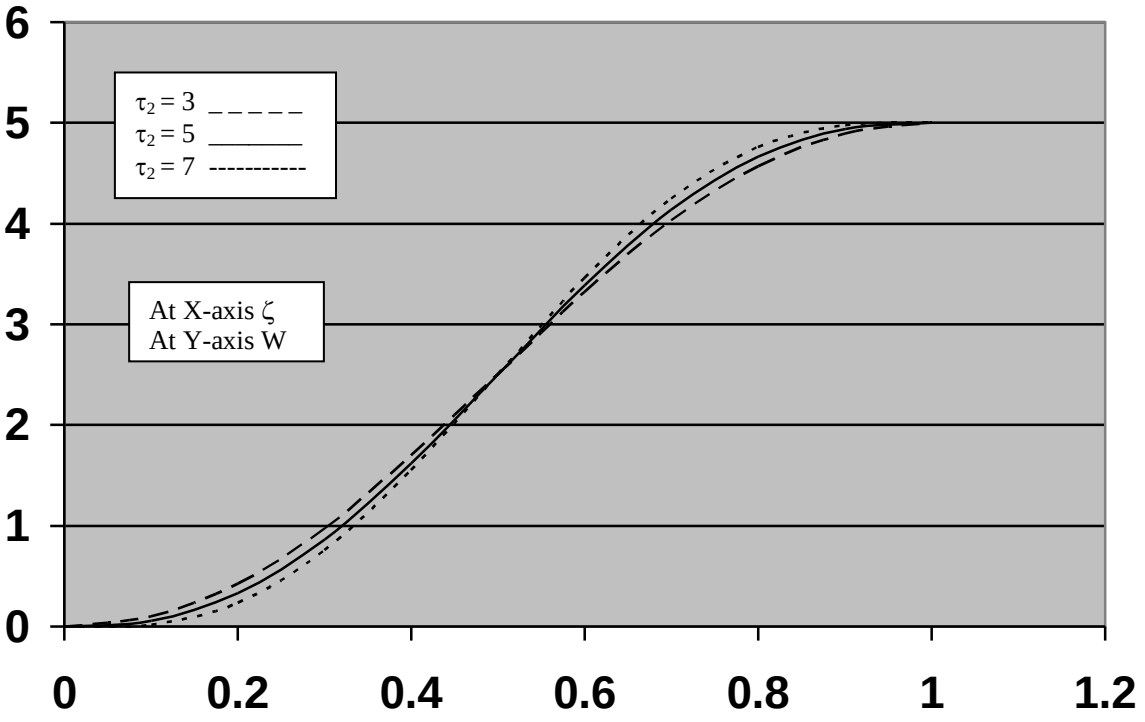

Fig. 6 Response of axial velocity to an increase in elastico-viscous effects.

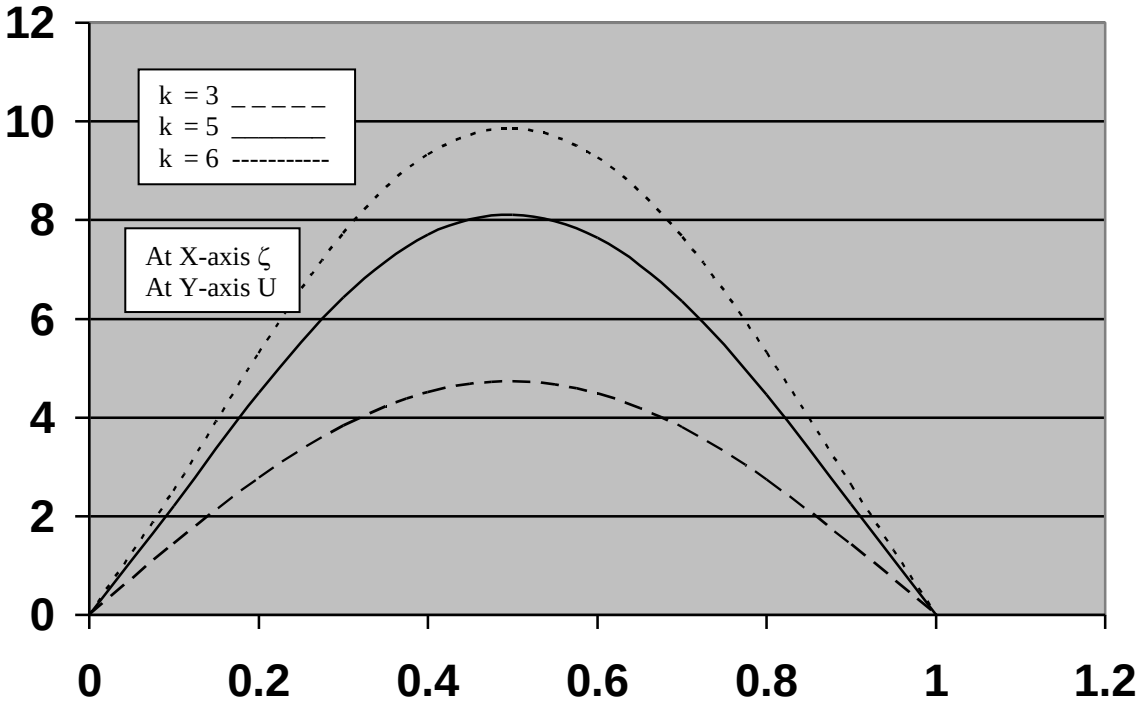

Fig. 7 Response of radial velocity with injection.

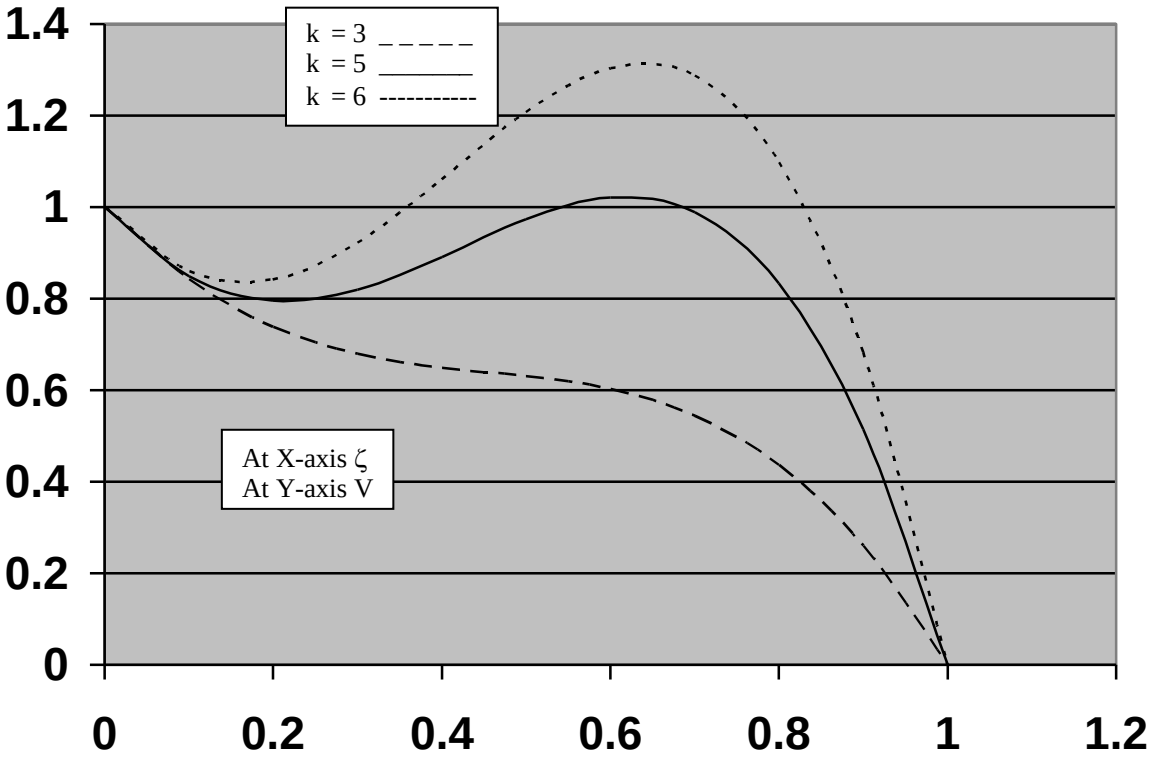

Fig. 8 Response of transverse velocity with injection.

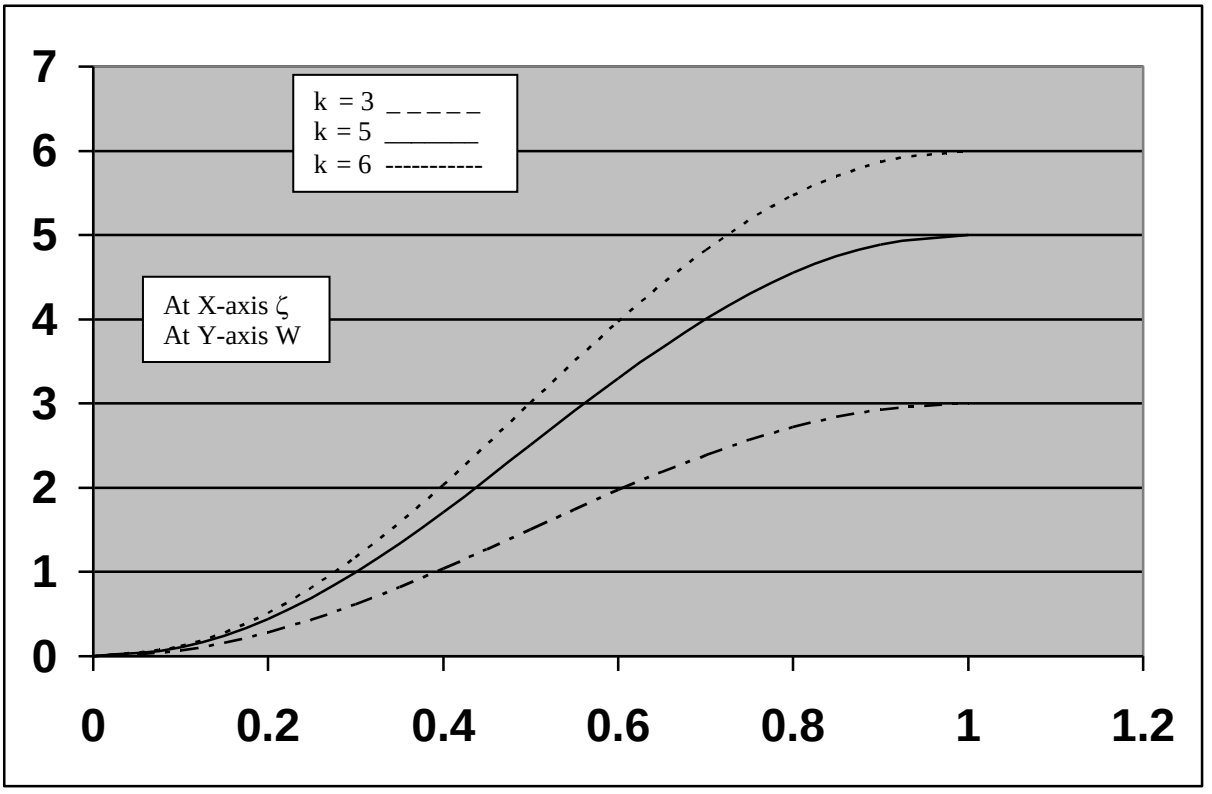

Fig. 9 Response of axial velocity with injection.

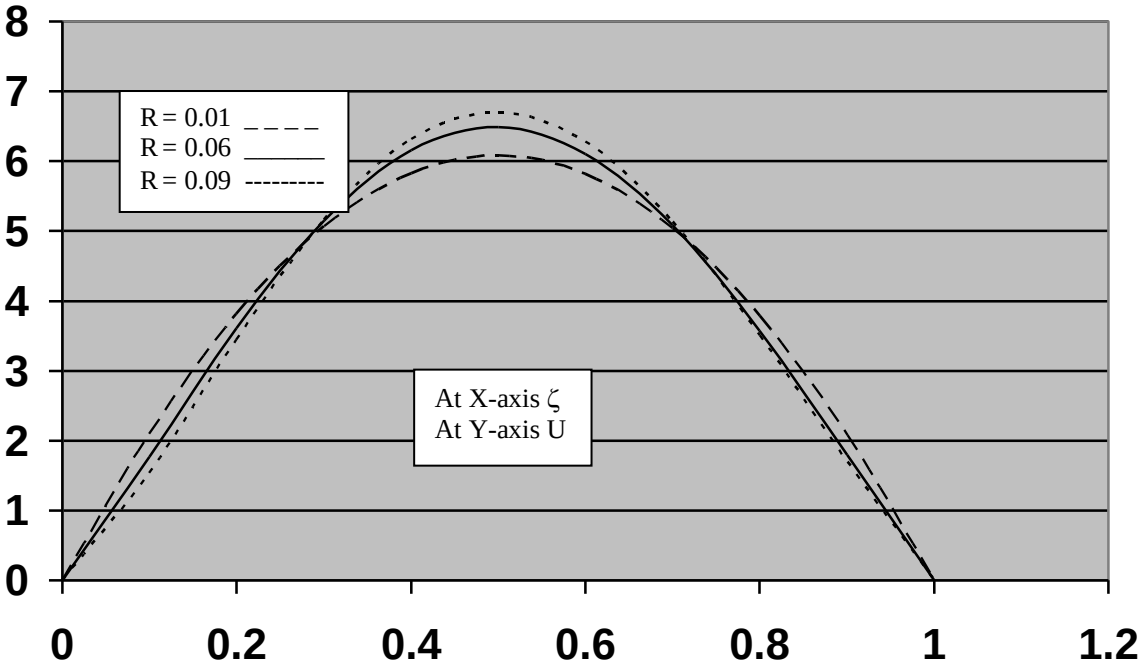

Fig.10 Response of radial velocity with different Reynolds number.

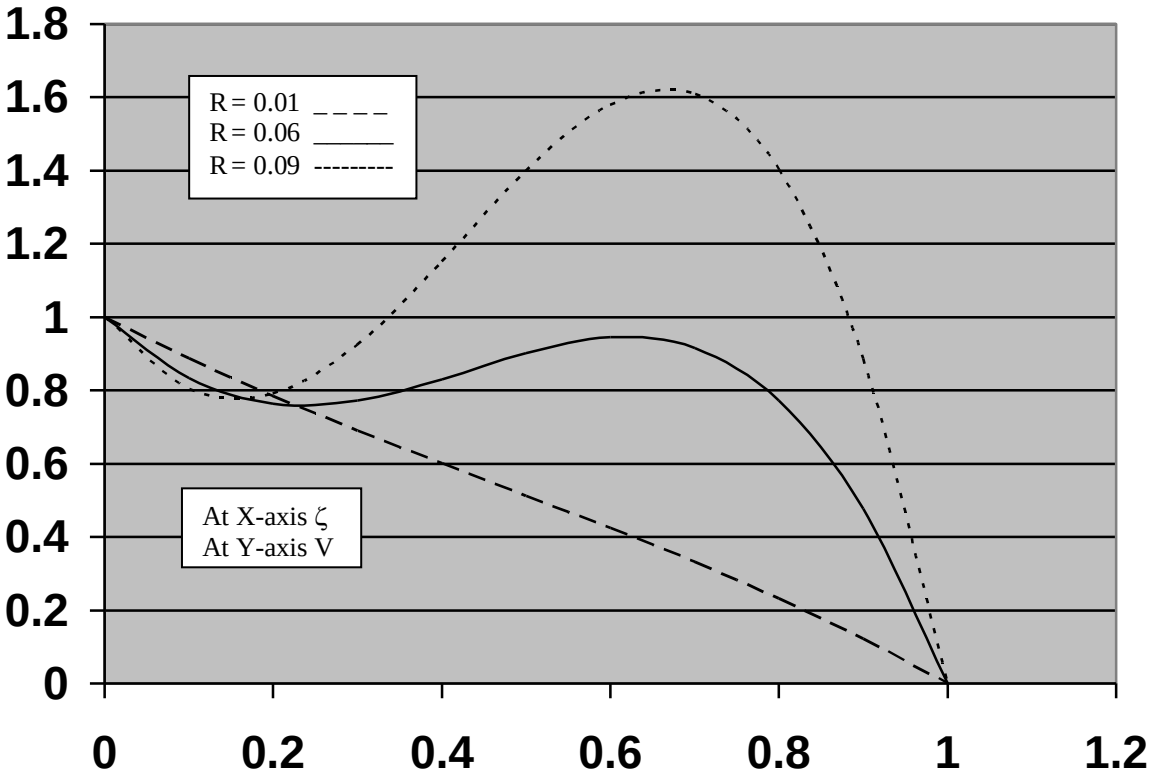

Fig.11 Response of transverse velocity with different Reynolds number.

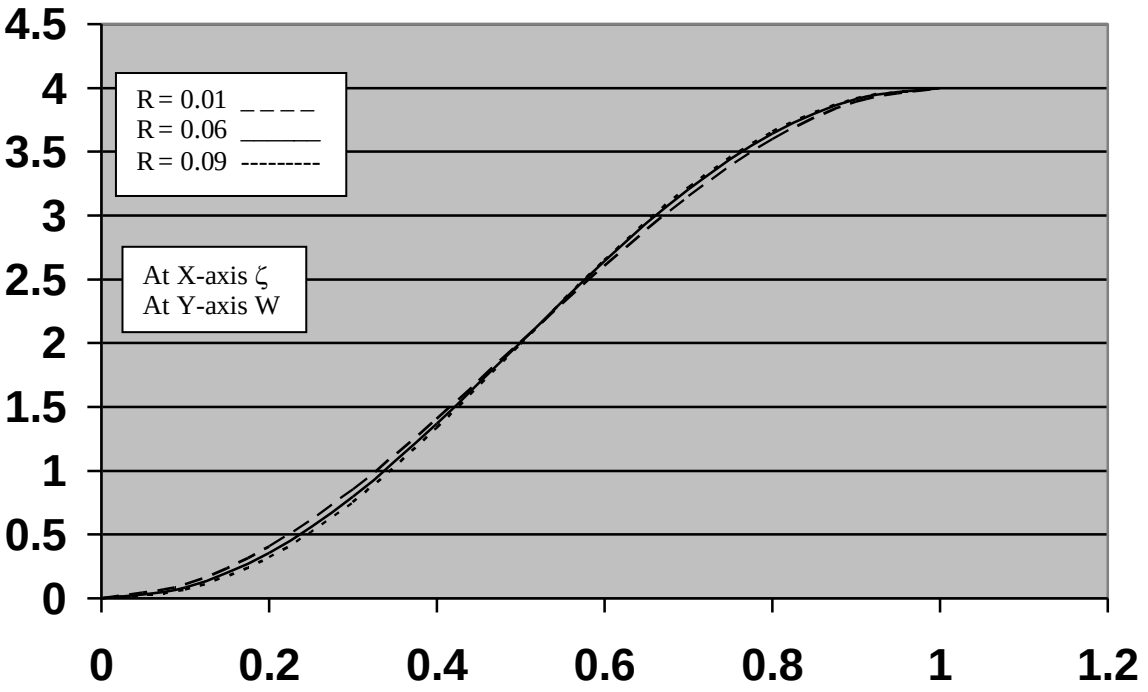

Fig. 12 Response of axial velocity with different Reynolds number.

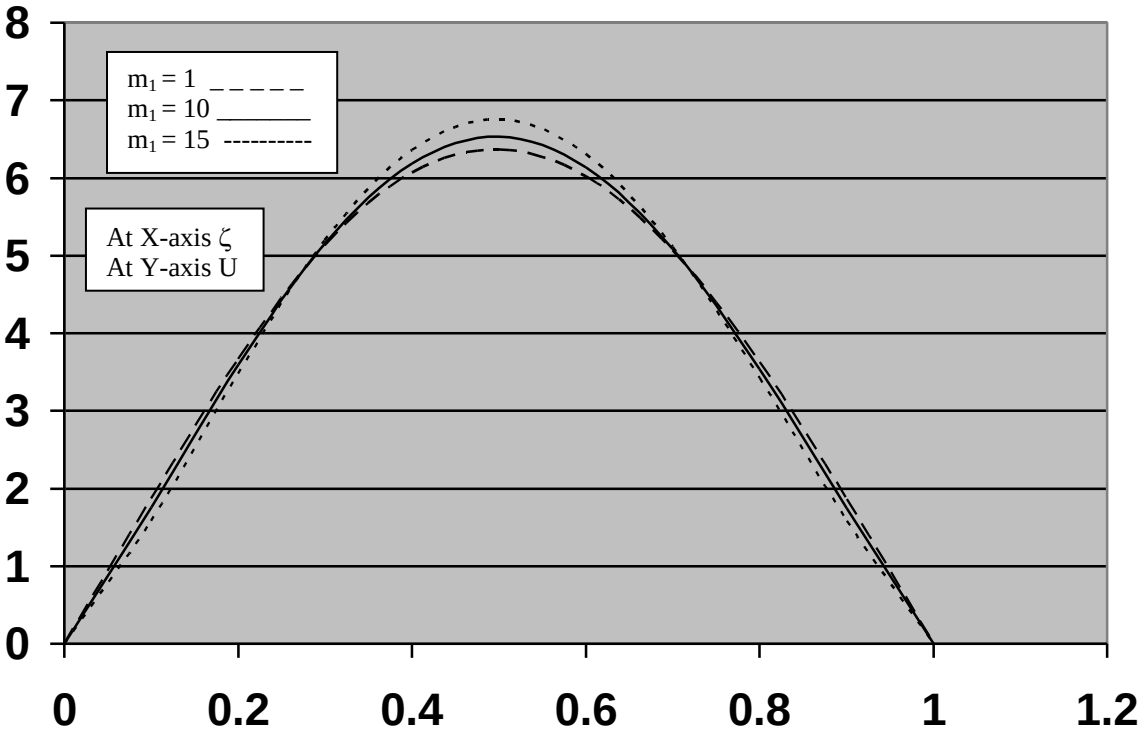

Fig.13 Response of radial velocity with different m_1.

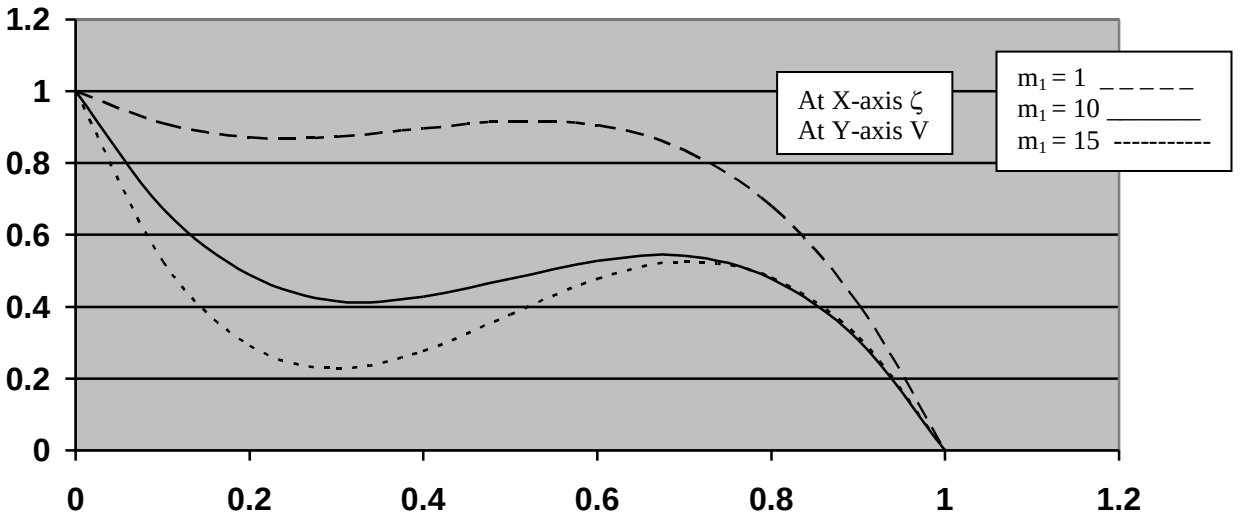

Fig.14 Response of transverse velocity with different m_1.

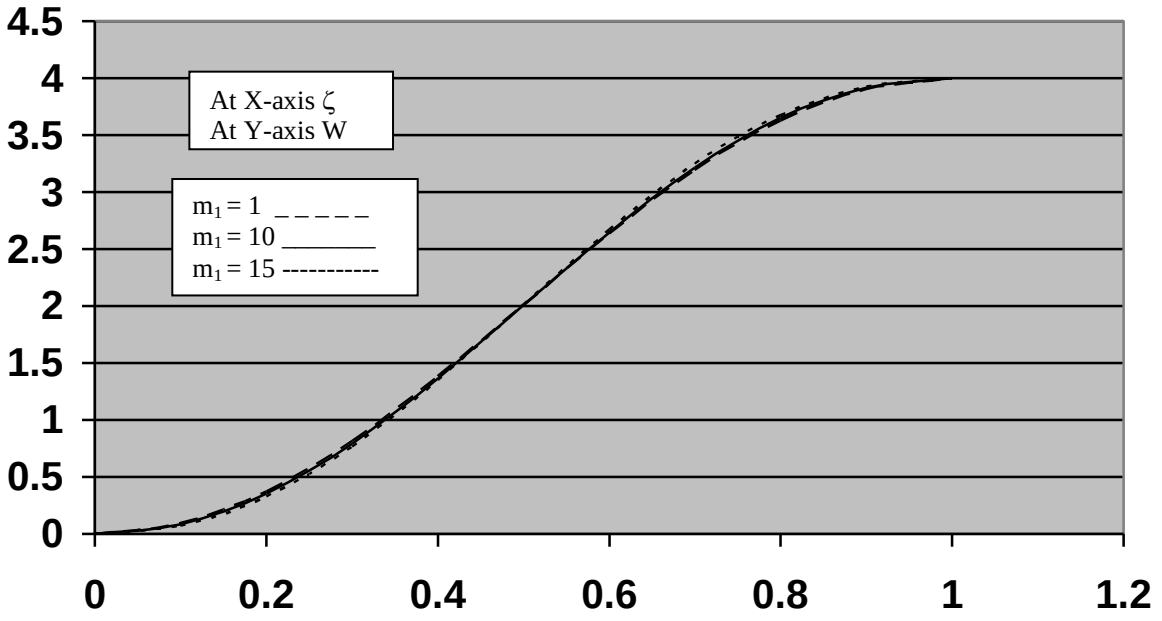

Fig.15 Response of axial velocity with different m_1.

IV. REFERENCES

[1] Sharma, H.G. and D.S. Gupta, Ind. J. Pure App. Math. 14(1983)1091.
[2] K. R. Rajgopal, J.Non-Newtonian Fluid Mech. 9 (1981)
[3]H. G. Sharma & K. R. Singh, Indian J. Pure & appl. Math. 17(7), (1986), 931.
[4] Khare Sadhna, Indian J. Pure & appl. Math. 8 (1977), 808-815.
[5] B. B. Singh & Anil Kumar, Indian J. Pure & appl. Math., 20(9), 931-943,(1989)
[6]Coleman, .D. and W.Noll, Arch. Rat'l. Mech. Anal., 6(1960) 355.
[7]A. C. Srivastava, J. Fluid Mech. 17(1963), 171.
[8]L. O. Wilson & N. L. Schyer, J. Fluid Mech. 85 (1978), 479.
[9] T. Van Karman. Z. angew Math. Mech. 1 (1921), 232.